Ablation of smooth muscle myosin heavy chain SM2 increases smooth muscle contractility and results in postnatal death in mice

Mei Chi*, Yingbi Zhou*, Srikanth Vedamoorthyrao, Gopal J. Babu & Muthu Periasamy

Department of Physiology and Cell Biology, College of Medicine and Public Health, The Ohio State University, 304 Hamilton Hall, 1645 Neil Ave, Columbus, Ohio 43210

Short title: SM2 & smooth muscle contraction

* Both authors contributed equally to the work

Corresponding Address:

Muthu Periasamy, PhD
Department of Physiology and Cell Biology
The Ohio State University College of Medicine
304 Hamilton Hall
1645 Neil Ave
Columbus, OH 43210
Phone: 614-292-2310
Fax: 614-292-4888
Email: periasamy.1@osu.edu

The smooth muscle myosin heavy chains (SMHC) are motor proteins powering smooth muscle contraction[1-4]. Alternate splicing of SHMC gene at the C-terminus produces SM1, and SM2 myosin isoforms; SM2 (200 kDa) contains a unique 9-amino-acid sequence at the carboxyl terminus, whereas SM1 (204 kDa) has a 43 amino acid non-helical tail region[5-7]. To date the functional difference between C-terminal isoforms has not been established; therefore, we used an exon-specific gene targeting strategy and generated a mouse model specifically deficient in SM2. Deletion of exon-41 of the SMHC gene resulted in a complete loss of SM2 in homozygous ($SM2^{-/-}$) mice, accompanied by a concomitant down-regulation of SM1 in bladders. While heterozygous ($SM2^{+/-}$) mice appeared normal and fertile, $SM2^{-/-}$ mice died within 30 days after birth. The peri-mortal $SM2^{-/-}$ mice showed reduced body weight, distention of the bladder and alimentary tract, and end-stage hydronephrosis. Interestingly, strips from $SM2^{-/-}$ bladders showed increased contraction to K^+ depolarization or M3 receptor activation. These results suggest that SM2 myosin has a distinct functional role in smooth muscle, and the deficiency of SM2 increases smooth muscle contractility, and causes dysfunctions of smooth muscle organs, including the bladder that leads to the end-stage hydronephrosis and postnatal death.

We and others have previously shown that alternate splicing of the SMHC gene at the N- and C-terminus produces four isoforms (SMA/B, SM1/2) that are restricted to the smooth muscle lineage[5-8]. During embryonic development in mice, SM1 appears early by 10.5 days post-coitum, whereas SM2 appears late in fetal development around birth and increases steadily during the postnatal stages; reaching a SM1 to SM2 ratio of 1:1 in

adult stages[9]. The ratio of SM2:SM1 is both tissue- and species-specific, and is altered during disease states; decreased expression of SM2 has been found in primary pulmonary hypertension, in neointimal smooth cells of injured or/and atherosclerotic vessels, and in obstructive bladder disease[10-14]. Studies also suggest that an alteration in SM2 : SM1 ratio could modify force development[15-18]. In the present study, we used an exon-specific gene-targeting strategy to generate a mouse model that is deficient in SM2 but continues to express SM1. To ablate SM2 , exon-41 encoding nine c-terminal amino acids, a stop signal, along with its flanking 5'and 3' splicing sequences was replaced with a neomycin-resistance cassette under the HSV-TK promoter in the reverse orientation in a targeting vector (Fig.1 A). Successful targeting and germ-line transmission was confirmed by long-distance PCR analyses using primers specific for the wild-type (WT), and mutant alleles (data not shown). Both heterozygous ($SM2^{+/-}$) and homozygous ($SM2^{-/-}$) pups were delivered in an expected Mendelian ratio, which suggests that loss of SM2 does not result in embryonic lethality.

The homozygous newborns had normal body size at birth; however by day 20, the $SM2^{-/-}$ mice showed a significant decrease in body weight compared to the $SM2^{+/+}$ mice (8.88 ± 0.35 g vs. 15.61 ± 1.2 g; $P < 0.001$) and about ~ 50% of the homozygous mice died during the first two weeks. Mice that survived beyond two weeks showed enlargement of the gastrointestinal system, distention of the bladder, enlarged kidneys (due to development of hydronephrosis) and retention of urine in the bladder (Fig 1B). All homozygous $SM2^{-/-}$ mice died within 4 weeks after birth but the heterozygous mice appeared normal and were able to breed. The peri-mortal $SM2^{-/-}$ mice showed severe urinary retention in the renal pelvis and bladder body, and developed end-stage

hydronephrosis. We also found that the bladder body of peri-mortal $SM2^{-/-}$ mice was significantly enlarged, but its wall thickness was reduced (Fig 1B and C). On the other hand, the morphology of the cardiovascular system including aorta and the heart was not affected in $SM2^{-/-}$ mice (data not shown). These results indicate that SM2 is essential for the in vivo function of the bladder and alimentary tract.

To understand the molecular bases for the observed phenotype, we determined if protein expression was altered by deletion of the SM2-specific exon. Samples from neonate bladders from mice 4-7 days of age, a stage where the $SM2^{-/-}$ bladder was not distended, were examined. Quantitative Western blot analysis showed that SM2 protein was absent in $SM2^{-/-}$ bladder as expected and in the $SM2^{+/-}$ bladder, its expression level was decreased by 20% (Fig 2A). Also, there was a decrease in the level of SM1 in $SM2^{+/-}$ and $SM2^{-/-}$ bladder (27% and 56%, respectively; Fig 2A). On the other hand, the levels of α-SM-actin and tropomyosin were not altered. Total SMHC protein as assessed by Coomassie-blue staining of the gel was decreased by 16% and 62% in $SM2^{+/-}$, and $SM2^{-/-}$ bladder, respectively (Fig 2A). However, the SMHC protein band density in aorta was very similar between $SM2^{-/-}$ and $SM2^{+/+}$ mice (Fig 2A), which suggests that the decrease in SM1 level in $SM2^{+/-}$ and $SM2^{-/-}$ bladders represents an adaptive response to the loss of SM2. Furthermore, electron microscopic examination of the bladder sections showed that the overall morphology and structure of smooth muscle cells were similar between null and $SM2^{+/+}$ mice. These results suggest that deletion of the SM2 exon selectively alters thick filament proteins, and does not affect the overall smooth muscle cell structure in mouse bladder.

Next, we determined if the deficiency of SM2 myosin affected smooth muscle contraction by examining isometric force development in isolated neonatal bladder muscle strips. As shown in Fig 3A, while $SM2^{+/-}$ strips showed responses to K^+ comparable with that of $SM2^{+/+}$ mice, whereas those of $SM2^{-/-}$ mice responded to K^+ with a significantly increased sustained-phase of maximal contraction (689 ± 35 mg vs. 242 ± 26 mg or 84.3 ± 3.0 % vs. 28.4 ± 2.8 % of peak value at 60 mM K^+, $P< 0.001$; Fig 3B) and a significantly reduced EC_{50} (concentration of K^+ to reach 50% of maximal contraction; 20.4 ± 0.4 vs. 42.9 ± 0.4 mM; $P<0.001$). Similarly, in response to a sub-maximal (1 μM) concentration of Carbachol, a selective agonist of the M3 receptor that controls physiological bladder emptying, the $SM^{-/-}$ strips also showed significantly enhanced contraction (105.6 ± 1.4 % and 74.4 ± 3.8 % vs. 49.3 ± 4.1 % and 27.8 ± 5.0% in peak and sustained force, respectively; $P<0.001$) compared to that of $SM^{+/+}$, (Fig 2A). These results altogether suggest that the complete loss of SM2 myosin increases smooth muscle contractility, whereas a partial loss of SM2 could be compensated in the presence of a concomitant decrease in SM1.

To further explore the mechanisms responsible for increased contractility in $SM2^{-/-}$ bladders, we determined the Ca^{2+} sensitivity of contractile apparatus in bladder muscle strips. As shown in Fig 3B, compared to that of $SM^{+/+}$ mice, the pCa^{2+}-force relationship in β-esin permeabilized $SM2^{-/-}$ strips was significantly shifted to the left (EC50: 0.93 ± 0.02 vs. 1.70 ± 0.15 μM; $P < 0.001$; Fig 3B). This result suggests that the loss of SM2 increases the intrinsic Ca^{2+} sensitivity of the contractile apparatus. Since phosphorylation of the regulatory myosin light chain (MLC20) is the initiator of cross-bridge cycling, and normally correlates with the force generation in smooth muscle contraction[19], we

determined if this was altered in $SM2^{-/-}$ bladders. To this end, muscle strips were stimulated with 40 mM K^+, at which a contraction near to maximum was developed in $SM2^{-/-}$, but only 30-40% in $SM^{+/+}$ mice. As shown in Figure 4, the ratios of phosphorylated to total MLC20 both in resting strips and those treated with 40 mM K^+ were similar between $SM^{+/+}$ and $SM^{-/-}$ strips. This result suggests that loss of SM2 does not alter the steady state level of MLC20 phosphorylation and as a result, it is most likely that the loss of SM2 directly affects the properties of cross-bridge cycling and force generation during smooth muscle contraction.

The above results suggest that SM2 myosin function distinctly from the other SHMC isoform, i.e. SM1, and an appropriate ratio of SM1and SM2 myosin is essential for the normal contractility of smooth muscle in organs, such as the bladder. In support of this idea, the ablation of SMHC gene, (total loss of SMHC protein) resulted in a drastic decrease of smooth muscle contraction [20]. In addition, the loss of SM2 in $SM^{+/-}$ or $SM^{-/-}$ bladders was accompanied by a concomitant decrease of SM1. $SM^{+/-}$ bladder (despite a decrease in SM2) developed comparable force to that of $SM^{+/+}$ mice. This further underscores a unique role for SM2, and suggests that in smooth muscle there exists a mechanism to maintain a constant ratio of SM1 and SM2. A recent study also showed that the SM1 and SM2 ratio was not changed by transgenic over-expression of either SM1 or SM2; while the transgenic protein was expressed, it was offset by a decrease in the levels of endogenous SM1 or SM2 proteins in the mouse bladder [18].

Also of note is that in the presence of increased smooth muscle contractility, $SM2^{-/-}$ mice showed urinary retention in bladder or/and the renal pelvis. This might reflect an

increased urinary flow resistance, as observed in obstructive diseases. SM2 has been found to be unevenly distributed among smooth muscle tissues. For example, in the urethra, SM2 is more abundant than in the bladder[21]. Thus, it remains to be further understood how the ablation of SM2 affects muscle function in the ureter and urethra or the functional coordination between organs involved in the in vivo regulation of urinary emptying.

In summary, in this study we generated a mouse model specifically deficient in SM2. Our results suggest that SM2 myosin has a distinct function and is necessary for overall smooth muscle contractility. Furthermore ablation of SM2 results in hypercontractility of smooth muscle but causes dysfunction of smooth muscle organs, including the bladder that leads to development of end-stage hydronephrosis and postnatal death.

Methods

Generation of SM2-deficient mice

Genomic fragment of SM-MHC gene containing the 3' region (20 kb) was isolated from a λ/129 mouse genomic library. Exon 41 and its 5'and 3' splicing sites (0.4 kb) were replaced with a neomycin-resistance cassette under the HSV-TK promoter in reverse orientation. The linearized construct was electroporated into mouse 129 embryonic stem cells. Clones resistant to neomycin were screened by long-distance PCR with primers specific for the wild type allele and mutant allele. Targeted clones were injected into C57BL/6 blast cysts. Chimeric males were mated to B6 females, and the germ line transmission of targeted allele was detected by long-distance PCR. $SM2^{-/-}$ were obtained by cross-breeding of $SM2^{+/-}$ mice.

Tissue preparation

Neonate mice (4-7 days) were used for the experiments. Bladders were isolated and cut open, and the mucosa was removed by dissection under a binocular microscope. For the functional analyses, muscles from the front wall were cut transversally into 1 mm wide and 2 mm long strips. The strips were tied with thread filaments to form a loop at both ends separated by a distance of 1 mm. In some experiments the thoracic aortas were also isolated and dissected free of adherent tissues for protein analyses.

Analyses of protein expression

Protein expression was analyzed with western blot as described elsewhere[22]. Briefly, crude myofibril proteins isolated from bladder muscle were separated by electrophoresis on SDS-PAGE (5% for SM2 and SM1; 10% for α-actin and tropomyosin;

15% for MLC20), and transferred to a nitrocellulose membrane. Proteins were sequentially probed with respective first and secondary antibodies. Anti-SM1 and Anti-SM2 antibodies were kindly provided by Dr. AF Martin and Dr. R Nagai, respectively. Anti-α-actin and anti-MLC20 antibodies were purchased from Sigma (St Louis, MO). In some experiments, the SDS-PAGE (10%) gels were stained with Coomassie-blue to directly visualize both SMHC and actin. Band densities were quantified and analyzed with a Biochemi System (UVP, Upland, CA).

Electron Microscopic examination

The bladders were expanded in situ and fixed with 4% glutaraldehyde in 0.1M phosphate buffer (PH7.2). Strips cut from the treated bladders were further post-fixed in 2% OsO_4 for 2 hrs at room temperature, and contrasted in saturated uranyl acetate for 4 h at 60 ^{o}C. Samples were embedded in Epon 812 and cut into sections, which were stained with uranyl acetate and lead. Images were detected and photographed with an electron microscope (EM 410; Philips Electron Optics, Mahwah, NJ).

Analysis of intact bladder smooth muscle function

Muscle strips were attached with the loops to two tungsten wires in an organ bath (3 ml) filled with physiological salt solution[23](PSS) maintained at 37^{o}C. One wire was fixed, and the other was connected to a force transducer (AE801, Holten, Norway). Tissues were set at 1.5 times resting length (at which length the contractile response to 60 mM K^+ was maximal and reproducible), and the contractions to the subsequent 10-50 mM K^+ or Carbachol (1 μM) were determined sequentially. Force was expressed as a percentage of peak value evoked by 60 mM K^+.

Myofilament Ca^{2+} sensitivity

Muscle strips were attached to the force apparatus as described above, and set at to 1.5 times resting length at room temperature. The strips were permeabilized with 50 μM β-esin (40 min) in Ca^{2+}-free cytosolic substitution solution (CSS^{24}), and treated with 10 μM A23129 (10 min) in Ca^{2+}-free CSS. After washout, strips were exposed to free Ca^{2+}-containing CSS (0.3-10 μM). Force development at each Ca^{2+} point was expressed as a percentage of maximal contraction obtained with 10 μM Ca^{2+}.

Measurement of MLC20 phosphorylation

Muscle strips (1 x 2 mm^2) were placed in 37°C PSS or 40 mM K^+ for 5 min and the reactions were stopped with 90% acetone, 10% trichloroacetic acid and 10 mM dithiothreitol (DTT) chilled at -80°C. Proteins were extracted, separated on Urea/glycerol gel (with the amount adjusted to achieve similar total MLC20 content between $SM2^{+/+}$ and $SM2^{-/-}$ mice), and transferred onto a nitrocellulose membrane as described previously[24]. Phosphorylated and un-phosphorylated MLC20 were probed with anti-MLC20 antibody, as in western blot analyses.

Statistics

For statistical evaluation, values were presented as mean ± SE. Comparison of two means was performed by unpaired Student's *t* test. Where more than two means were compared, 1-way or 2-way ANOVA followed by Dunnett's or Bonferroni's post hoc test was used. $P < 0.05$ was considered to be statistically significant.

Acknowledgement

This work was supported by NIH grant HL 38355-17 to MP. MC has been supported by an American Heart Association Postdoctoral Fellowship Grant (Ohio Valley) and YZ by an American Heart Association Scientist Development Grant. The authors are grateful to Drs. Sumei Liu and Jackie Wood for expert help with tissue morphology, and Drs Jack Rall, Jonathan Davis and Poornima Bhupathy for critical reading of the manuscript.

References

1. Rovner, A.S., Murphy, R.A. & Owens, G.K. Expression of smooth muscle and nonmuscle myosin heavy chains in cultured vascular smooth muscle cells. *J Biol Chem* **261**, 14740-14745 (1986).

2. Murphy, R.A., Walker, J.S. & Strauss, J.D. Myosin isoforms and functional diversity in vertebrate smooth muscle. *Comp Biochem Physiol B Biochem Mol Biol* **117**, 51-60 (1997).

3. Loukianov, E., Loukianova, T. & Periasamy, M. Myosin heavy chain isoforms in smooth muscle. *Comp Biochem Physiol B Biochem Mol Biol* **117**, 13-18 (1997).

4. Craig, R. & Woodhead, J.L. Structure and function of myosin filaments. *Curr Opin Struct Biol* **16**, 204-212 (2006).

5. Nagai, R., Kuro-o, M., Babij, P. & Periasamy, M. Identification of two types of smooth muscle myosin heavy chain isoforms by cDNA cloning and immunoblot analysis. *J Biol Chem* **264**, 9734-9737 (1989).

6. Nagai, R., Larson, D.M. & Periasamy, M. Characterization of a mammalian smooth muscle myosin heavy chain cDNA clone and its expression in various smooth muscle types. *Proc Natl Acad Sci U S A* **85**, 1047-1051 (1988).

7. Babij, P. & Periasamy, M. Myosin heavy chain isoform diversity in smooth muscle is produced by differential RNA processing. *J Mol Biol* **210**, 673-679 (1989).

8. Miano, J.M., Cserjesi, P., Ligon, K.L., Periasamy, M. & Olson, E.N. Smooth muscle myosin heavy chain exclusively marks the smooth muscle lineage during mouse embryogenesis. *Circulation research* **75**, 803-812 (1994).

9. White, S.L., Zhou, M.Y., Low, R.B. & Periasamy, M. Myosin heavy chain isoform expression in rat smooth muscle development. *Am J Physiol* **275**, C581-589 (1998).

10. Wang, Z.E., Gopalakurup, S.K., Levin, R.M. & Chacko, S. Expression of smooth muscle myosin isoforms in urinary bladder smooth muscle during hypertrophy and regression. *Lab Invest* **73**, 244-251 (1995).

11. Cher, M.L., Abernathy, B.B., McConnell, J.D., Zimmern, P.E. & Lin, V.K. Smooth-muscle myosin heavy-chain isoform expression in bladder-outlet obstruction. *World J Urol* **14**, 295-300 (1996).

12. DiSanto, M.E., *et al.* Alteration in expression of myosin isoforms in detrusor smooth muscle following bladder outlet obstruction. *Am J Physiol Cell Physiol* **285**, C1397-1410 (2003).

13. Packer, C.S., Roepke, J.E., Oberlies, N.H. & Rhoades, R.A. Myosin isoform shifts and decreased reactivity in hypoxia-induced hypertensive pulmonary arterial muscle. *The American journal of physiology* **274**, L775-785 (1998).

14. Aikawa, M., *et al.* Human smooth muscle myosin heavy chain isoforms as molecular markers for vascular development and atherosclerosis. *Circulation research* **73**, 1000-1012 (1993).

15. Malmqvist, U., Arner, A. & Uvelius, B. Contractile and cytoskeletal proteins in smooth muscle during hypertrophy and its reversal. *Am J Physiol* **260**, C1085-1093 (1991).

16. Gomes, C.M., *et al.* Improved contractility of obstructed bladders after Tadenan treatment is associated with reversal of altered myosin isoform expression. *The Journal of urology* **163**, 2008-2013 (2000).

17. Paul, R.J., Bowman, P.S., Johnson, J. & Martin, A.F. Effects of sex and estrogen on myosin COOH-terminal isoforms and contractility in rat aorta. *Am J Physiol Regul Integr Comp Physiol* **292**, R751-757 (2007).

18. Martin, A.F., *et al.* Expression and function of COOH-terminal myosin heavy chain isoforms in mouse smooth muscle. *Am J Physiol Cell Physiol* **293**, C238-245 (2007).

19. Somlyo, A.P. & Somlyo, A.V. Ca2+ sensitivity of smooth muscle and nonmuscle myosin II: modulated by G proteins, kinases, and myosin phosphatase. *Physiol Rev* **83**, 1325-1358 (2003).

20. Morano, I., *et al.* Smooth-muscle contraction without smooth-muscle myosin. *Nature cell biology* **2**, 371-375 (2000).

21. Hypolite, J.A., *et al.* Regional variation in myosin isoforms and phosphorylation at the resting tone in urinary bladder smooth muscle. *Am J Physiol Cell Physiol* **280**, C254-264 (2001).

22. Babu, G.J., *et al.* Loss of SM-B myosin affects muscle shortening velocity and maximal force development. *Nature cell biology* **3**, 1025-1029 (2001).

23. Zhou, Y., Dirksen, W.P., Babu, G.J. & Periasamy, M. Differential vasoconstrictions induced by angiotensin II: role of AT1 and AT2 receptors in isolated C57BL/6J mouse blood vessels. *Am J Physiol Heart Circ Physiol* **285**, H2797-2803 (2003).

24. Zhou, Y., Hirano, K., Sakihara, C., Nishimura, J. & Kanaide, H. NH2-terminal fragments of the 130 kDa subunit of myosin phosphatase increase the Ca2+ sensitivity of porcine renal artery. *J Physiol* **516 (Pt 1)**, 55-65 (1999).

Figure Legend

Figure 1: SM2 gene-targeting strategy and mouse phenotype. *A:* Representation of exon 41-specific (SM2 isoform-specific) gene targeting. Exon 41 and its flanking sequences were replaced with neomycin gene in reverse orientation. *B:* Phenotype of $SM2^{-/-}$ mice; top: bladder (1), alimentary tract (2) including stomach (3), and the kidney (4) in $SM^{+/+}$ and $SM^{-/-}$ mice (20 days); Bottom: end-stage hydronephrosis in 25-day $SM2^{-/-}$ and kidneys in age-matched $SM2^{+/+}$ mice, *C:* Top: comparson of neonatal and peri-mortal $SM2^{-/-}$ with age-match $SM^{+/+}$ bladders. Bottom: microscopic examination of peri-mortal $SM2^{-/-}$ and age-matched $SM2^{+/+}$ bladders.

Figure 2: Muscle protein expression and smooth muscle cell structure. *A:* top: Western blot analyses of SM1 and SM2. *Middle:* Western blot analyses of a-actin and tropomysin. *Bottom:* Commassie blue staining of gel showing the total SMHC and actin. *B:* Morphology and structure of bladder smooth muscle cells detected with electron microscopy.

Figure 3: Analyses of bladder smooth muscle contractility. *A:* Representative traces from 5-7 experiments showing the contraction of intact smooth muscle from bladders of $SM^{+/+}$ (blue), $SM2^{+/-}$ (green), or/and $SM2^{-/-}$ (red) mice to 60 mM K^+ with subsequent 10-50 mM K^+ (top) or 1 μM Carbachol (bottom). *B:* Representative traces (top) and summary (bottom) of the responses induced by 0.3 to 10 μM Ca^{2+} in β-escin (50 μM) permeabilized $SM^{+/+}$ (blue) and $SM2^{-/-}$ (red) strips.

Figure 4: Detection of phosphorylated and unphosphorylated MLC20 in resting (PSS) and 40 mM K^+ (K^+) stimulated smooth muscle of $SM2^{+/+}$ (blank bar) and $SM^{-/-}$ (filled bar) bladders (n = 4).

Figure 1

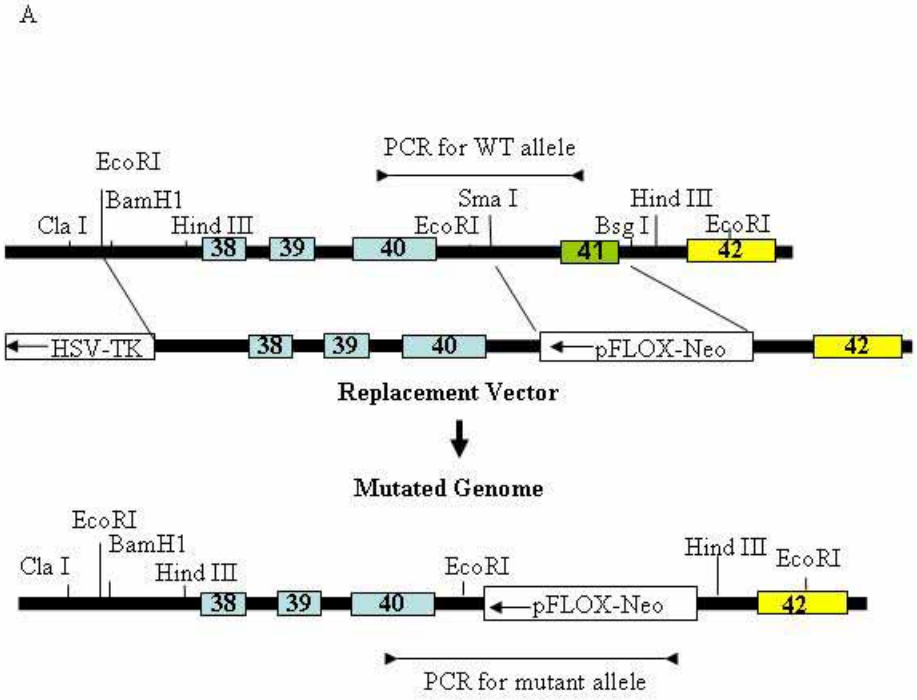

Figure 1

B

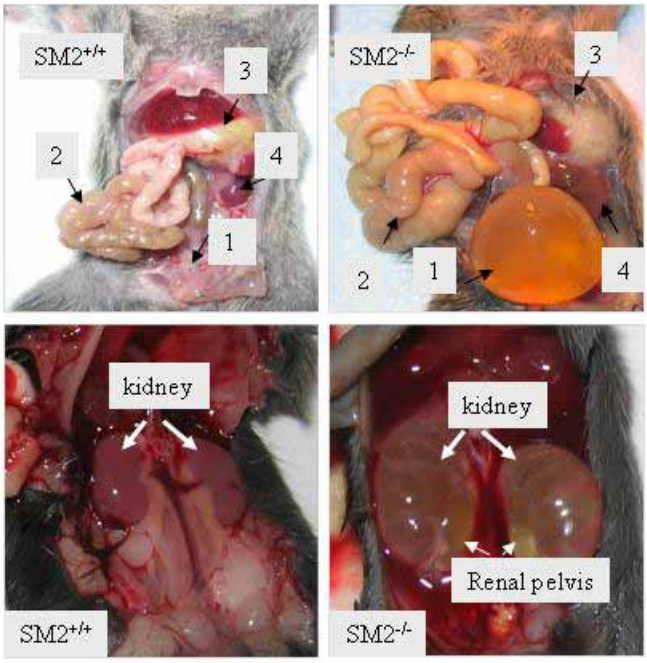

Figure 1

C

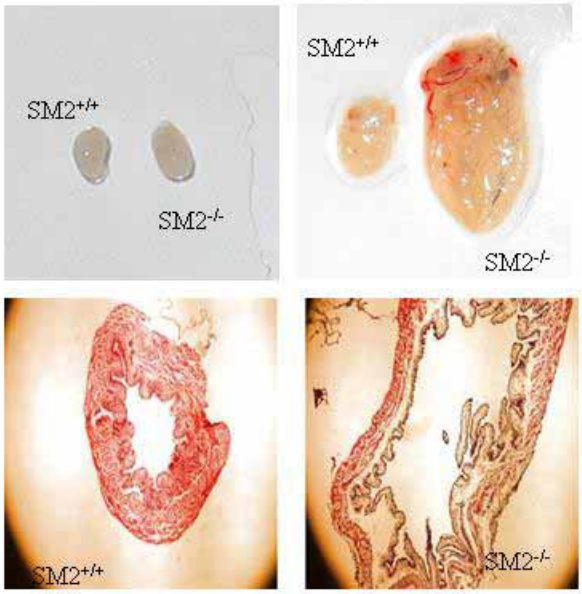

Figure 2

A

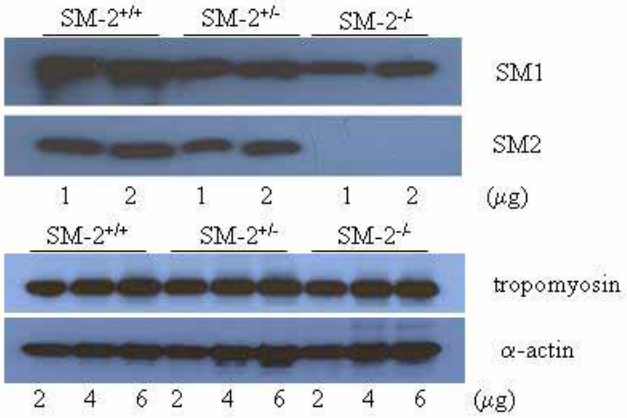

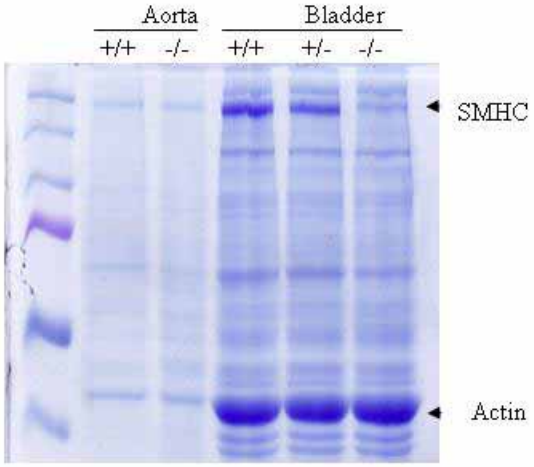

Figure 2

B

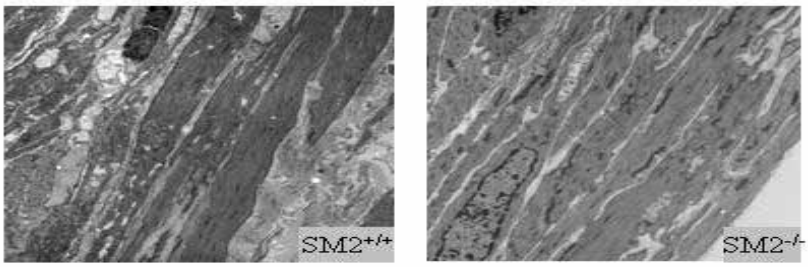

Figure 3

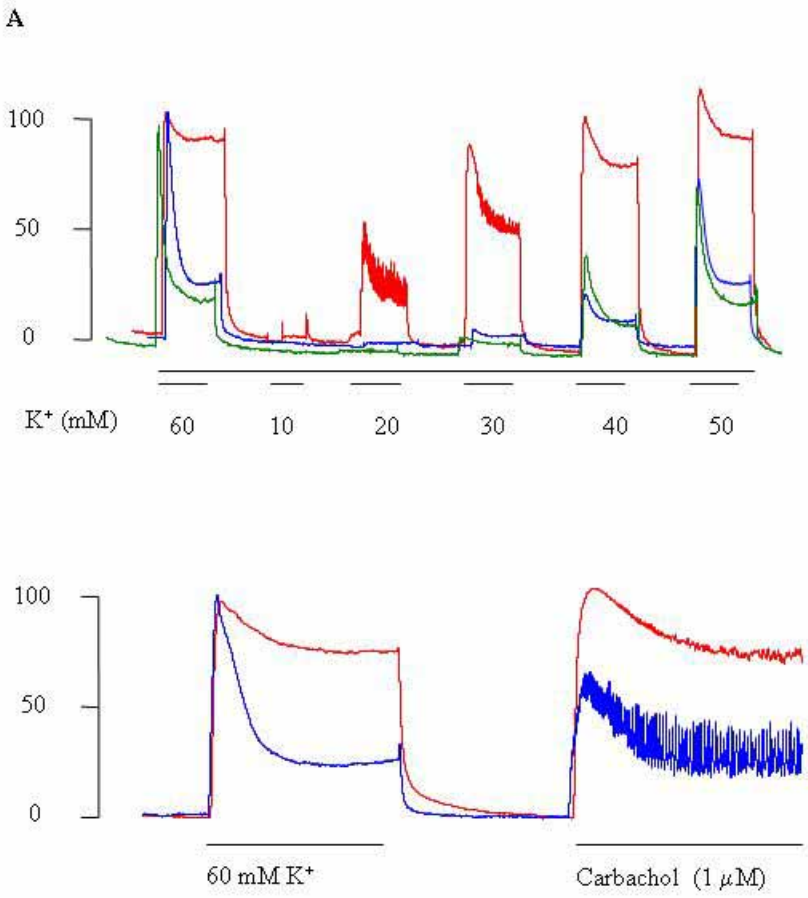

Figure 3

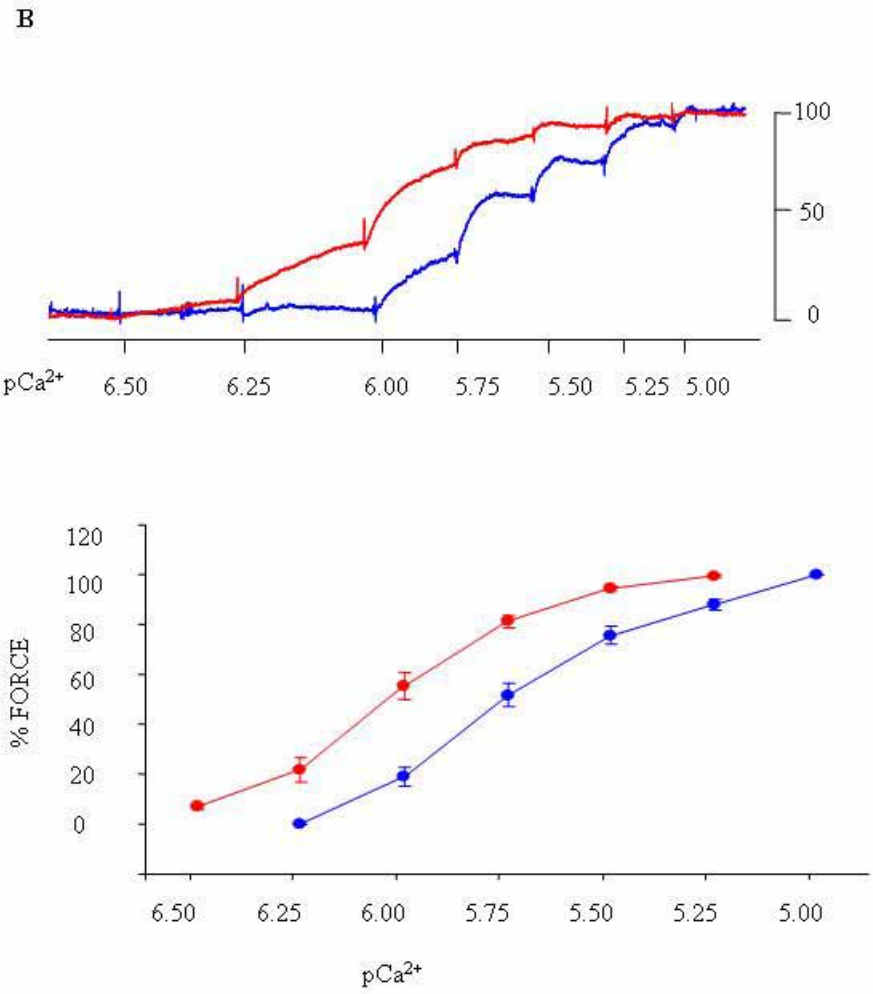

Figure 4